Additive-Free Dispersion of Single-Walled Carbon Nanotubes and Its Application for Transparent Conductive Films

ARTICLE *in* ADVANCED FUNCTIONAL MATERIALS · JUNE 2011

Impact Factor: 11.81 · DOI: 10.1002/adfm.201002257

ADVANCED FUNCTIONAL MATERIALS
www.afm-journal.de

Materials Views
www.MaterialsViews.com

Additive-Free Dispersion of Single-Walled Carbon Nanotubes and Its Application for Transparent Conductive Films

Wen-Bin Liu, Songfeng Pei, Jinhong Du, Bilu Liu, Libo Gao, Yang Su, Chang Liu, and Hui-Ming Cheng**

A good dispersion of single-walled carbon nanotubes (SWCNTs) in liquid media is a prerequisite to fulfill many of their applications. This contribution reports an efficient approach to additive-free dispersion of SWCNTs with the aid of functionalized carbonaceous byproducts (CBs, e.g., amorphous carbon, carbon nanoparticles, and carbonaceous fragments) in SWCNT products. SWCNT bundles are treated by oleum intercalation and nitric acid oxidation in sequence, which leads to the selective functionalization of the CBs while the structure and properties of the SWCNTs are well preserved. These functionalized CBs can improve the subsequent dispersion of SWCNTs and the majority of SWCNTs in the suspension are present in small bundles or individually. Moreover, SWCNT transparent conductive films (TCFs) are fabricated by using these suspensions. The SWCNT TCFs obtained can achieve a low sheet resistance of 76 and 133 Ω sq^{-1}, with optical transmittance of 82% and 90% at 550 nm, respectively.

1. Introduction

Single-walled carbon nanotubes (SWCNTs) have been attracting considerable scientific interest due to their unique one-dimensional structure and exceptional electronic, thermal, and mechanical properties, which endow them with great potential in various applications.[1,2] A good dispersion of SWCNTs in liquid media is a prerequisite to fulfill many of these promising applications.[3] However, due to strong van der Waals interactions between adjacent SWCNTs (~500 eV μm^{-1}) and extremely high aspect ratio (typically >1000), SWCNTs have a strong tendency to form large bundles, which severely limits their properties and applications in many fields.[4,5] Generally, there are three major strategies to disperse SWCNTs in aqueous and commonly-used organic solvents, i.e., noncovalent functionalizations,[6–13] covalent functionalizations,[4,14] and sovlent exfoliation.[15–18] These three strategies have their own advantages and disadvantages. For example, noncovalent functionalization by adsorption and wrapping of certain additives such as surfactants,[13] polymers,[10] DNA,[6–8,11,12] and peptides[9] is regarded as most promising for the dispersion of SWCNTs without degrading their intrinsic properties. However, these additives are usually insulating and difficult to remove completely, which results in additional electrical resistance at inter-tube junctions.[19] Covalent chemical functionalization, on the other hand, does not need additives, but it modifies the sp^2 carbon framework of SWCNTs to a certain degree, thus inevitably altering their intrinsic properties.[4,14] Solvent exfoliation is used for the dispersion of SWCNTs in certain solvents with no additives or functionalization.[15] However, such solvents, e.g., N-methyl-2-pyrrolidone (NMP),[17] N, N-Dimethylform (DMF),[16] *o*-dichlorobenzene (DCB),[20] and dichloroethane (DCE)[18] either possess high boiling points[16,17,20] or are toxic,[18,20] which hinders their feasibility in practical manipulation.[21] Therefore, to extract the full potential of SWCNTs for many applications, a method capable of effectively dispersing SWCNTs in low boiling point and low toxicity solvents without degrading the intrinsic properties of SWCNTs and without the need of external additives is highly desired.

Herein, we report an approach to obtain soluble SWCNTs which can be spontaneously dispersed in aqueous and common low boiling point organic solvents without the aid of additives and more importantly, with the preservation of the intrinsic structure and properties of the SWCNTs. This SWCNT dispersion method can be regarded as additive-free with respect to surfactant, polymer, and DNA-based wrapping methods. These additive-free SWCNT suspensions can be used in many fields. As an example, transparent conductive films (TCFs) were fabricated using the SWCNT suspensions, and they have a low sheet resistance of 76 and 133 Ω sq^{-1} with optical transmittance of 82% and 90% at 550 nm, respectively. These films are expected to have a good potential in electronic and optoelectronic devices.

W.-B. Liu, S. F. Pei, Dr. J. H. Du, B. L. Liu, L. B. Gao, Y. Su, Prof. C. Liu, Prof. H.-M. Cheng
Shenyang National Laboratory for Materials Science
Institute of Metal Research
Chinese Academy of Sciences
72 Wenhua Road, Shenyang 110016, P. R. China
E-mail: cheng@imr.ac.cn jhdu@imr.ac.cn

DOI: 10.1002/adfm.201002257

2. Results and Discussion

2.1. Basic Principle and Preparation of SWCNT Dispersion

Our idea arises from the fact that there are some carbonaceous byproducts (CBs), e.g., amorphous carbon, carbon nanoparticles,

and carbonaceous fragments, during the synthesis of SWCNTs.[22–25] These CBs are usually amorphous or have low crystallinity and consequently, they are more chemically reactive or have lower chemical and thermal stability than high-quality SWCNTs with better structural perfection.[22,26] Due to the difference in chemical reactivity between CBs and SWCNTs, it is possible to realize the selective functionalization of CBs, while keeping SWCNTs less affected or even unaffected. This argument is validated by Green et al. who showed that nitric acid can create COOH functionality on the carbonaceous fragments and emphasized that the majority of the COOH groups are present on carboxylated carbonaceous fragments rather than on the side walls of SWCNTs.[26] Furthermore, Huang et al. recently demonstrated that graphene oxide can act as a surfactant to disperse graphite powder and multi-walled CNTs in water due to its amphiphilicity, the marked feature of surfactants, resulting from the hydrophilic edges and hydrophobic basal plane.[27] We speculate that once CBs are functionalized with COOH groups, they may also be amphiphilic and play the same role as surfactants in the dispersion of SWCNTs.

The preparation of soluble SWCNTs is schematically shown in **Figure 1**. The SWCNTs were synthesized by floating catalyst chemical vapor deposition (FCCVD),[28,29] and then purified by refluxing in 37% HCl to partly remove Fe catalyst nanoparticles. These as-purified SWCNTs are present as big bundles (usually 10–50 nm in diameter) with some carbonaceous substances firmly attached on their outer surface (Figure 1a and S1). It is reported that SWCNT bundles can be intercalated, disentangled, and dissolved in superacids such as oleum or chlorosulphonic acid.[4,30–32] In this work, the as-purified SWCNT soot was selectively oxidized by oleum intercalation and nitric acid treatment in sequence to obtain the soluble SWCNTs. The oleum intercalation treatment decreases the interaction between adjacent SWCNTs and causes SWCNT bundles to swell. This provides channels for oxidizing agents to infiltrate the bundles and expose the CBs (Figure 1b). By controlling oxidation conditions, our treatment largely preserves the structural integrity and high intrinsic electrical conductivity of the SWCNTs, while the CBs can be functionalized with COOH groups. These functionalized CBs, which attached tightly on the surface of the SWCNTs (Figure 1c), can act as amphiphilic surfactants owing to their hydrophobic carbon framework and hydrophilic COOH groups and render the SWCNTs soluble in solvents.

2.2. Optimization of Experimental Conditions for Soluble SWCNTs

To optimize experimental conditions and achieve a good dispersion of SWCNTs, many factors including oxidation temperatures, SWCNT/oleum ratios, and oleum intercalation temperatures were investigated. Here, we fixed the oleum/HNO_3 ratio at 3:1 (*V*/*V*) (**Table 1**), the same as that used in a recent work,[4] since the mixture of concentrated sulfuric and nitric acids at the ratio of 3:1 (*V*/*V*) is widely used for the oxidation of CNTs.[33–37] We found that the oxidation temperature of the as-purified SWCNTs in oleum-HNO_3 is one of the most important factors for preparing the soluble SWCNTs: if the oxidation temperature is higher than 95 °C, the majority of SWCNTs is consumed by the acids; if the oxidation temperature is lower than 60 °C, the obtained SWCNTs are not soluble. Therefore, the optimized temperature for the selective oxidation is 70 ± 5 °C. Another important process that affects the final dispersion of SWCNTs is the oleum intercalation. Generally, the reagent/intercalant ratio and the intercalation temperature are believed to affect the intercalation process.[38] To optimize the dispersion of soluble SWCNTs, these two factors were carefully considered by varying SWCNT/oleum ratios

Table 1. Soluble SWCNT samples prepared from different conditions. The oxidation temperature of all the as-purified SWCNTs in oleum-HNO_3 was controlled at 70 ± 5 °C.

Soluble SWCNTs	SWCNTs [mg]	Oleum [mL]	HNO_3 [mL]	Intercalation temperature [°C]	Absorbance at 400 nm in water
Sample 1	50	60	20	25	0.46
Sample 2	50	60	20	80	0.49
Sample 3	50	60	20	120	0.50
Sample 4	50	15	5	25	0.87
Sample 5	50	15	5	80	0.91
Sample 6	50	15	5	120	0.97
Sample 7	50	30	10	25	1.10
Sample 8	50	30	10	80	1.26
Sample 9	50	30	10	120	1.38

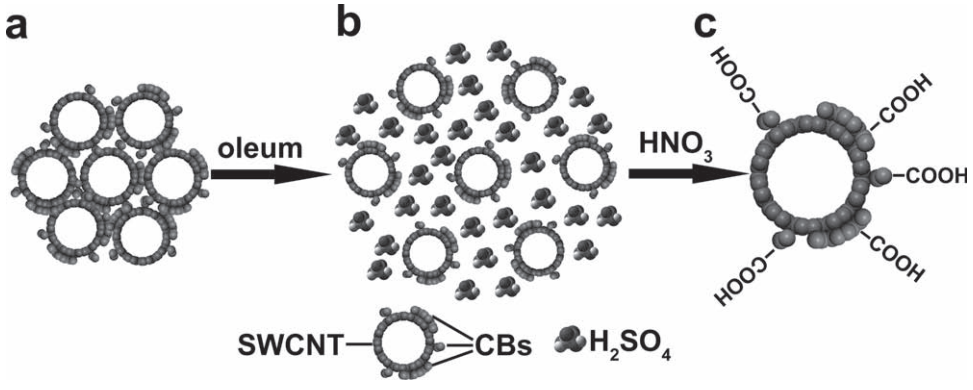

Figure 1. Schematic of the preparation of soluble SWCNTs: a) tightly bundled SWCNTs, b) oleum intercalated SWCNT bundle, and c) a soluble SWCNT.

and the intercalation temperatures (Samples 1 to 9, as listed in Table 1). After intercalation and oxidation of the as-purified SWCNTs in sequence, black SWCNT slurries were collected. All these slurries can be dissolved spontaneously in water and commonly-used polar organic solvents (e.g., ethanol, acetone, and isopropanol), which are attractive since they have a low boiling point, high volatility, and low toxicity. **Figure 2**a shows a sequence of photographs (taking Sample 9 as an example at 0 min, 10 min, 1 h, and 2 days) of the spontaneous dissolution process after adding water to a cuvette containing the SWCNT slurry without any sonication or stirring.

Atomic force microscopy (AFM) was used to evaluate the dispersion state of the soluble SWCNTs prepared under different conditions (suspensions of Samples 1 to 9). As shown in Figure 2b and S2, the majority of SWCNTs in the suspensions are present in small bundles or individually (detailed statistic data will be given in the next section) and no obvious difference is observed in the bundle/tube height distribution of soluble SWCNTs, indicating a similar dispersion state of these soluble SWCNTs in the suspensions. This may be due to the fact that only small bundles or individual SWCNTs can be dissolved spontaneously in water and the commonly-used polar organic solvents. Moreover, the optical absorption spectroscopy was used to demonstrate the dispersion efficiency of the soluble SWCNTs in suspensions. We measured optical absorption spectra by adding 50 mL water into each soluble SWCNT sample and compared their absorbance at 400 nm, as shown in **Figure 3** and Table 1. Since the initial amount of as-purified SWCNTs was fixed at 50 mg under different treatment conditions and the absorbance is regarded as proportional to the concentration of SWCNTs,[39] we can directly compare the concentration of the soluble SWCNTs in these suspensions using the absorption intensity. A higher absorbance indicates a higher concentration of soluble SWCNTs and thus higher dispersion efficiency. From Figure 3, we observed that all the absorption spectra of the SWCNT suspensions are smooth and featureless, owning to heavy doping of SWCNTs by acids and strong background arising from the functionalized CBs.[40] We also observed that, at a fixed SWCNT/oleum ratio, a higher intercalation temperature can give rise to a slightly higher concentration of soluble SWCNTs. Nevertheless, the SWCNT/oleum ratios have a greater influence on the final dispersion efficiency of SWCNTs than the oleum intercalation temperature. The higher concentration of soluble SWCNTs can be obtained for a SWCNT/oleum ratio of 50 mg/30 mL than for other SWCNTs/oleum ratios. After detailed comparisons, the optimized conditions for the preparation of soluble SWCNTs is the SWCNT/oleum ratio of 50 mg/30 mL at the intercalation temperature of 120 °C, and the subsequent soluble SWCNTs were prepared under these conditions.

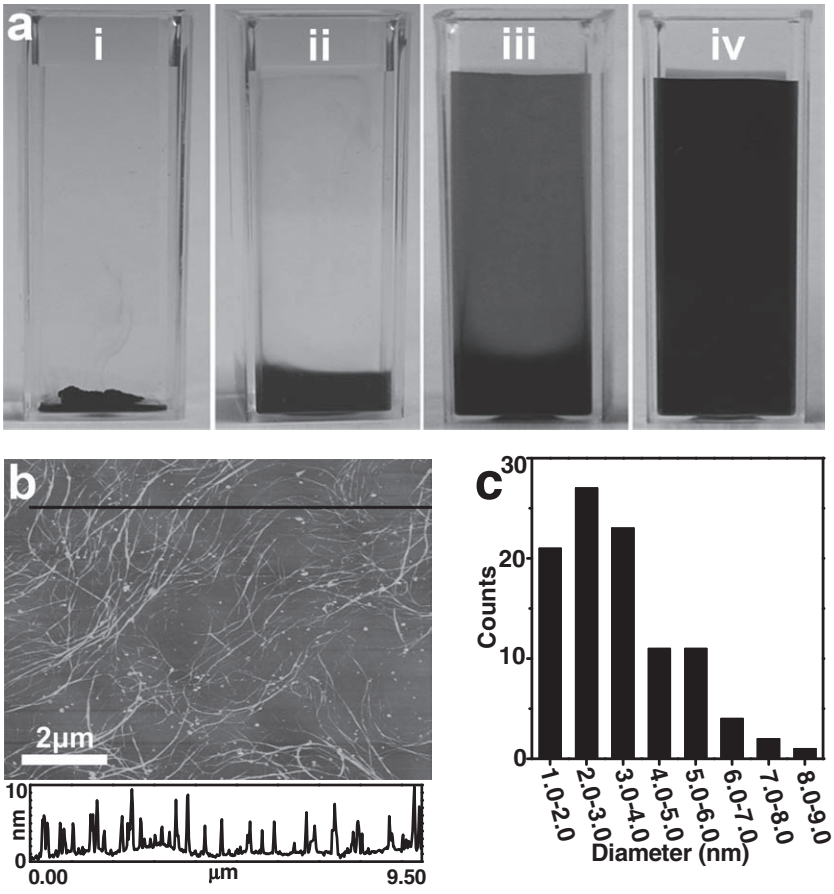

Figure 2. a) Photographs of dissolution of soluble SWCNTs in water, for i) 0 min, ii) 10 min, iii) 1 h, and iv) 2 days. b) Top panel: a typical AFM image of soluble SWCNTs in the cuvette iv) in a; lower panel: height profile of SWCNT bundles/tubes along the line in the top panel. c) Bundle/tube height distribution of the soluble SWCNTs.

2.3. Dispersion State and Structure Integrity of SWCNTs in Suspension

The suspension of soluble SWCNTs in water and commonly-used polar organic solvents is very stable. Figure S3 shows the SWCNT suspensions with a concentration of about 10 mg L^{-1} in water, ethanol, acetone, and isopropanol after standing for one month, showing no precipitation or flocculation of SWCNTs. All of the above stable solutions are optically transparent and homogenous in appearance. The stability of the suspensions was further substantiated by a time-dependent absorption spectroscopy (Figure S4), which shows little change over a month.

Figure 2b is a typical AFM image of the SWCNTs dispersed in Figure 2a (iv). The AFM image clearly shows that the length of the SWCNTs is several micrometers, similar to that of the original SWCNTs. In contrast to the common covalent chemical functionalization, which usually leads to severe shortening of SWCNTs with length ranging from tens[4] to hundreds[37] of nanometers, our treatment leads to no obvious cutting of the SWCNTs, indicating the preservation of their structural integrity. Moreover, AFM analysis shows the de-bundling of the SWCNTs. Statistical

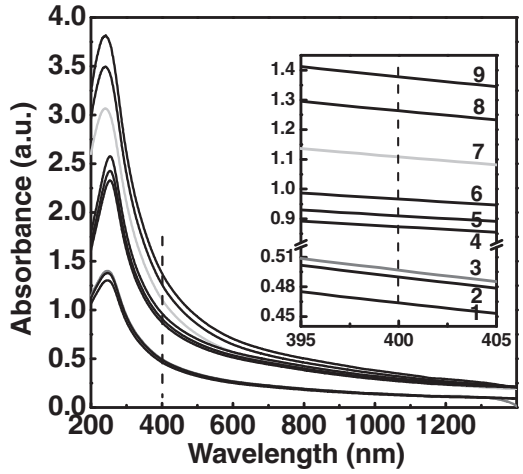

Figure 3. Absorption spectra of soluble SWCNTs in water from Samples 1 to 9 listed in Table 1. Inset: absorption spectra around 400 nm to show clearly the absorption intensity difference among these 9 samples.

analysis reveals that 93% of the bundles/tubes are smaller than 6 nm and that 48% of the bundles/tubes are smaller than 3 nm (Figure 2c and d). Note that our starting SWCNTs present as big bundles and have a diameter distribution in the range from 1.2 to 3.5 nm with a mean value of 2.1 nm from the high-resolution transmission electron microscopy (HRTEM) observation (Figure S1). As a result, we consider that the majority of soluble SWCNTs in the suspension are present in small bundles or individually, which is beneficial for applications requiring SWCNTs with both good dispersibility and high electrical conductivity.[41]

SEM characterization of our starting as-purified SWCNTs indicates that the SWCNTs are tightly entangled (**Figure 4**a). After a disentangling process using oleum, super ropes of ~200 nm in diameter were obtained (Figure 4b), which proves that oleum can act as an intercalating agent to render SWCNT bundles swollen.[32] The functionalized CBs attach on the SWCNTs, as shown in Figure 4c. The content of the functionalized CBs and SWCNTs in the soluble SWCNT slurry was estimated to be about 45 wt.-% and 35 wt.-% (detailed estimation in Supporting Information), respectively, according to thermogravimetric analysis/differential scanning calorimetric analysis (TGA/DSC) (Figure S5).

Raman spectroscopy and X-ray photoelectron spectroscopy (XPS) were used to study the quality of the SWCNTs during dispersion. The Raman spectra show the characteristic features of SWCNTs of a tangential G mode (~1590 cm^{-1}), a defect-induced D mode (~1320 cm^{-1}), and a radial breathing mode (RBM, at 100–300 cm^{-1}) (**Figure 5**a). The RBM of the as-purified SWCNTs shows multiple peaks (spectrum I in Figure 5a), corresponding to a wide diameter distribution of SWCNTs, which is consistent with the HRTEM results in Figure S1. It is worth noting that the diameter of the SWCNTs is much larger than that of two widely-used commercial SWCNTs: HiPCO (with diameter of 0.7–1.3 nm) and arc-discharge SWCNTs (with mean diameter of 1.38 nm).[42] After oleum and nitric acid treatment, the intensity of the RBM peak is dramatically decreased and the G band is blue shifted from 1589 to 1599 cm^{-1}, due to the strong p-type chemical doping by sulfuric and nitric acids.[43–45] The intensity ratio of the D peak to the G peak (I_D/I_G) has slightly increased from 0.1 for the as-purified SWCNTs to 0.2 for the soluble SWCNTs, indicating that some chemical functionalization is created during the oleum and nitric acid treatment. XPS analysis was performed to give additional proof regarding this chemical functionalization. The main C 1s peak of the as-purified SWCNTs is located at 284.4 eV, which is assigned to sp^2 carbon, with a tail near 285.0 eV for the sp^3 carbon.[46] The higher binding energy band between 287.0 and 292.0 eV corresponds to oxygen-related groups and the π–π* band (spectrum I in Figure 5b).[47] The appearance of the XPS peak with a binding energy of 288.5 eV in the soluble SWCNTs indicates a high concentration of COOH groups created in the sample (spectrum II in Figure 5b).

To further demonstrate the preservation of structural integrity of the SWCNTs and the functionalization of CBs, a heat treatment was carried out on the soluble SWCNTs, which is

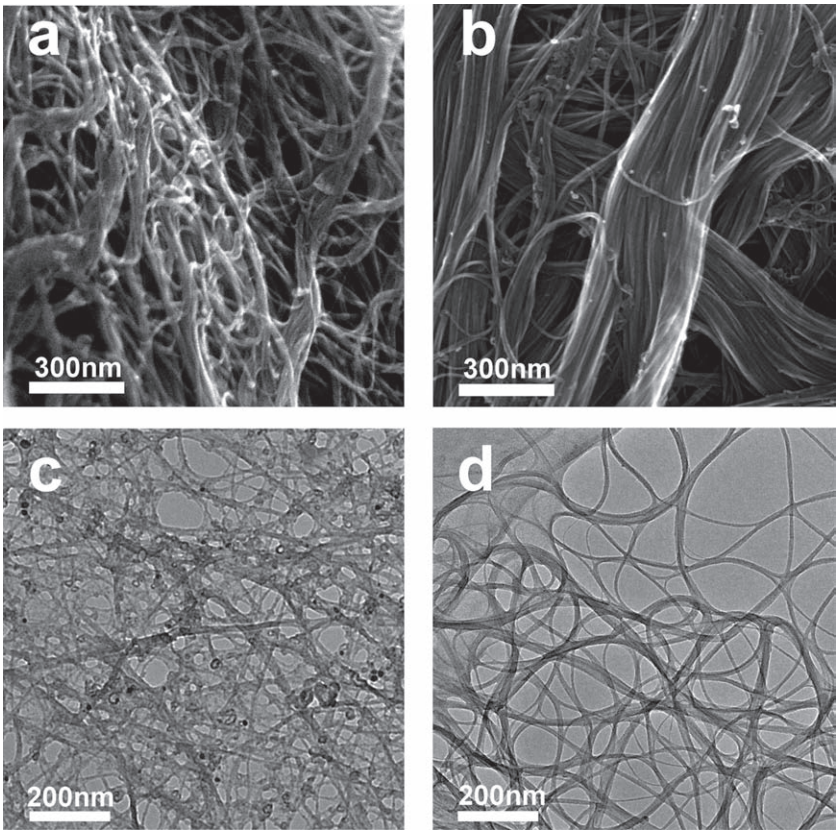

Figure 4. SEM images of a) tightly entangled network of the as-purified SWCNTs and b) ropes of SWCNTs after disentanglement by oleum intercalation. TEM images of c) the soluble SWCNTs and d) the SWCNTs from SWCNT TCFs after heat treatment and HCl immersion.

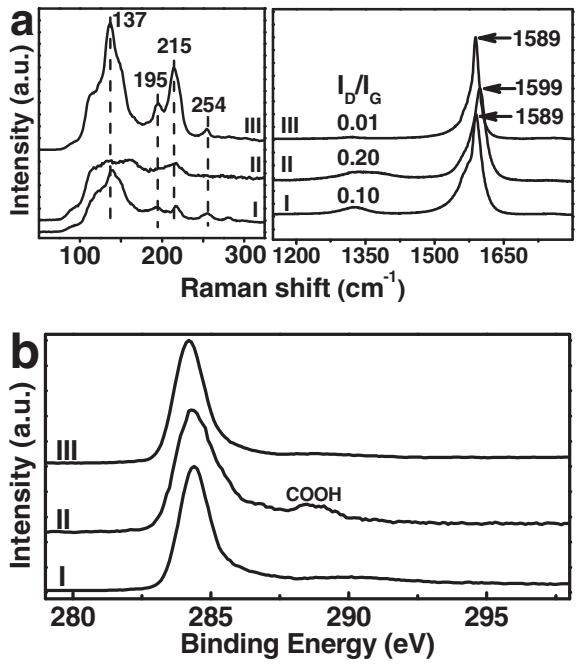

Figure 5. a) Raman and b) C1s XPS spectra of the SWCNTs: I) as-purified SWCNTs, II) soluble SWCNTs, and III) soluble SWCNTs after heating in air at 550 °C for 30 min. Raman spectra were normalized for equal intensity of the G band. The intensity decrease of RBM and the blue shift of G band in spectrum II originate from the chemical doping of SWCNTs by sulfuric acid and nitric acid. Heating treatment can eliminate the doping effect, thus the RBM and G band recover to their initial features, as shown in spectrum III.

effective in removing amorphous carbon[22,24] and also in eliminating chemical dopants.[48] After heating the SWCNT powder in air at 550 °C for 30 min, the Raman spectrum (spectrum III in Figure 5a) changes significantly. The RBM peaks recover their initial multiple peak features (comparing spectrum III with I in Figure 5a), and the intensity of the RBM peaks obviously increases. The G band returns to its initial position at 1589 cm^{-1}, and the I_D/I_G of the heat-treated SWCNTs decreases to 0.01, which is nearly ten times smaller than that of the as-purified SWCNTs. Furthermore, by comparing XPS spectrum III with I in Figure 5b, it is seen that the COOH groups are fully eliminated after heat treatment and the sp^2 carbon peak recovers to its initial state. Therefore, we believe that the COOH groups are mostly present in the CBs, while the SWCNTs are well preserved.

We have found that there are three key factors for determining whether the additive-free dispersion of SWCNTs can be obtained. (i) A certain amount of CBs contributes to the dispersion of SWCNTs. We found that soluble SWCNTs cannot be prepared if the as-produced SWCNTs were heated in air at 350 °C for 2 h before oleum and nitric acid treatment, since this step can burn out most of the CBs that were used for the SWCNT dispersion. (ii) The difference in chemical reactivity between CBs and SWCNTs is crucial for selective functionalization, which means that, under a certain oxidation condition, the SWCNTs can retain their intrinsic properties while the CBs are functionalized. (iii) It is very important to find a set of appropriate oxidation conditions, including oxidizing agents and reaction temperature, to achieve the selective functionalization of CBs, while keeping SWCNTs intact. In this work, the oxidation temperature was carefully controlled at 70 ± 5 °C by dropwise adding an oleum-SWCNT slurry to nitric acid.

2.4. Fabrication and Characterization of SWCNT TCFs

As stated above, a good dispersion of SWCNTs without perturbing their intrinsic properties and no external additives are highly desired for many applications. TCFs are important components in many electronic devices including touch screens, flat panel displays, photovoltaic cells, and organic light-emitting diodes.[49] SWCNT TCFs with good electrical conductivity and high flexibility have received much attention in recent years due to their potential for replacing indium tin oxides as transparent electrodes. We demonstrate here the fabrication of TCFs by using the additive-free dispersed SWCNTs. The SWCNT TCFs were fabricated on a glass or quartz substrate using a method similar to that developed by Wu et al.[49] A short time heat treatment was conducted on the as-prepared SWCNT TCFs to remove the functionalized CBs. After this, the sheet resistance of the heat treated TCFs was 180 Ω sq^{-1} with a transmittance of 80% at 550 nm and the color of the TCFs turned to faint yellow due to the oxidation of residual Fe nanopaticles, which can be easily removed by immersion in HCl. After HCl treatment, the transmittance was improved to 82%, and the sheet resistance was decreased to 147 Ω sq^{-1}, which can be attributed to slight HCl doping of the SWCNTs.[48] Figure 4d shows the TEM image of SWCNTs from the SWCNT TCFs after heat treatment and HCl immersion. An obvious difference from the soluble SWCNTs (Figure 4c) is that the agglomerated CBs and metal nanoparticles are effectively removed and the SWCNTs are well preserved, indicating that the functionalized CBs indeed exist in the soluble SWCNT sample and that their chemical and thermal stability is lower than that of SWCNTs. Chemical doping treatment by HNO_3 is a usual and effective method to improve the electrical conductivity of the SWCNT networks.[43,50,51] Figures 6a and b show the optical and SEM images of HNO_3-doped TCFs, which demonstrate a uniform and neat SWCNT network. The sheet resistance of the HNO_3-doped TCFs was decreased to 76 Ω sq^{-1}, while the transmittance of 82% had negligible change. We have also studied the thickness dependence of the sheet resistance and transmittance, as shown in **Figure 6**c. The thickness of the SWCNT films was measured by AFM at step edges (Figure 6e and f). The 62, 35, and 20 nm-thick SWCNT TCFs possess a sheet resistance of 48, 76, and 133 Ω sq^{-1} at optical transmittance of 73%, 82%, and 90%, respectively. To compare the performance of TCFs made from different materials, a figure of merit, the ratio of direct current conductivity (σ_{DC}) to the optical conductivity (σ_{OP}), is used.[52] It is suggested that a higher value of σ_{DC}/σ_{OP} indicates a better performance of TCFs.[41,53,54] Table S1 compares our result with the previous reported data for SWCNT TCFs and it can be seen that the TCFs prepared by using the additive-free SWCNT dispersion exhibit a better performance than most of other SWCNT TCFs. In addition, we used a surfactant (sodium

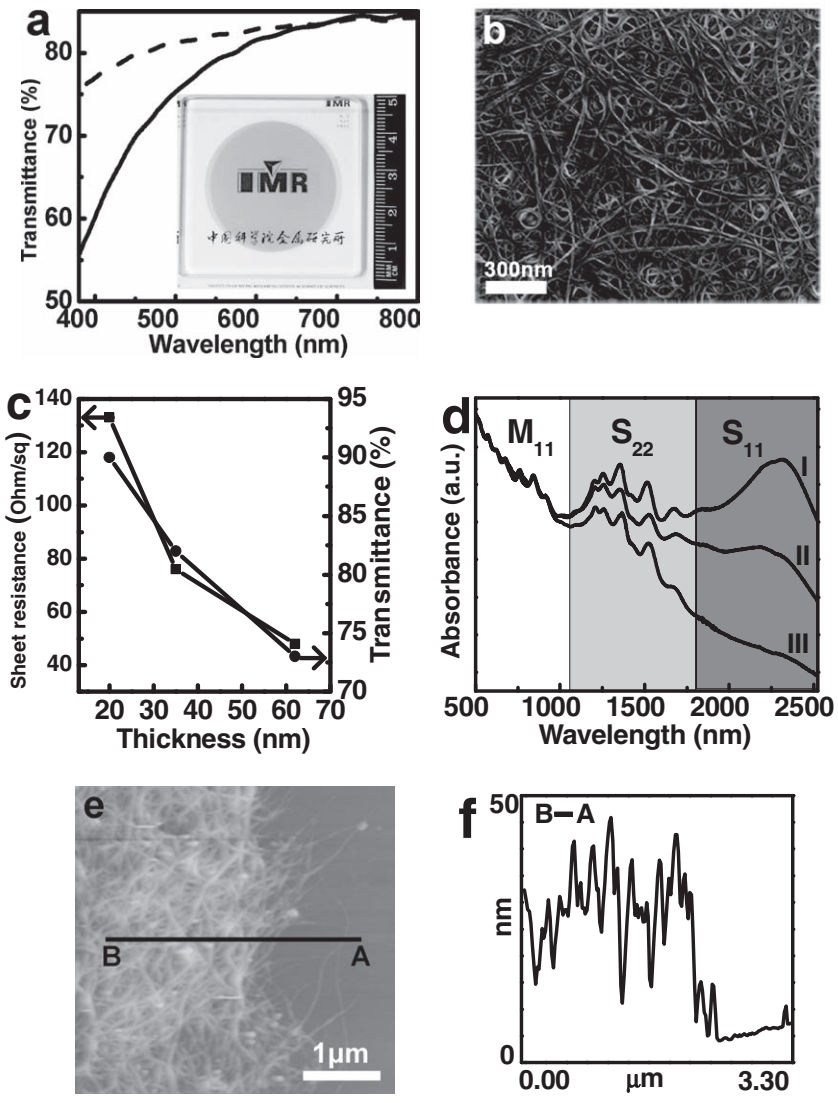

Figure 6. a) Transmittance spectra of the SWCNT TCFs before (solid line) and after (dash line) HCl immersion. Inset: an optical image of HNO_3-doped TCFs on a quartz substrate. b) A SEM image of SWCNT TCF. c) Sheet resistance and optical transmittance performance of SWCNT TCFs with different thicknesses. d) Optical absorption spectra of the SWCNT films: I) heat-treated, II) HCl-doped, and III) HNO_3-doped TCFs. e) AFM image of a transferred SWCNT film on a silicon wafer. f) Height profile along line AB in (e) showing a film thickness of ~35 nm.

dodecyl sulfate) aqueous solution to disperse the same kind of FCCVD-grown SWCNTs with the aid of ultrasonication for the preparation of TCFs in our previous work.[55] The sheet resistance of the obtained SWCNT TCFs with the best optical-electrical performance is 220 Ω sq^{-1} with an optical transmittance of 81% at 550 nm. It is obvious that the SWCNT TCFs obtained in this study have a better performance, indicating the advantages of our additive-free SWCNT dispersion method in the applications of SWCNT TCFs. Moreover, the sonication-free process which could be useful to reduce the shortening of SWCNTs during dispersion, also contributes to this better performance. Therefore, we consider that the good performance of SWCNT TCFs originates from the high quality and good dispersion state of SWCNTs in this study.

We further confirm the doping effects of HCl and HNO_3 on SWCNT TCFs by optical absorption spectroscopy (Figure 6d). After removal of the functionalized CBs by heat treatment, the characteristic bands of SWCNTs (spectrum I in Figure 6d) at around 2200, 1200 and 750 nm corresponding to S_{11} and S_{22} interband transitions in semiconducting SWCNTs, and M_{11} interband transitions in metallic SWCNTs are observed.[56,57] Moreover, the fine structures of the M_{11} and S_{22} interband transitions give additional evidence that the SWCNTs are present as small bundles or individually in the SWCNT TCFs.[13,58] Note that there are obvious changes in the S_{11} and S_{22} interband transitions caused by HCl or HNO_3 treatment. This can be attributed to the shift in Fermi level due to p-type doping of SWCNTs by HCl or HNO_3.[44] The S_{11} and S_{22} interband transitions of HNO_3-doped TCF were much more suppressed than those of HCl-doped TCF (comparing spectrum II with III in Figure 6d), indicating that HNO_3 has a stronger doping effect than HCl.[48]

3. Conclusion

In summary, we developed an efficient approach to prepare additive-free dispersions of SWCNTs with the aid of functionalized CBs. The CBs tightly attached on the side walls of SWCNTs can be selectively functionalized by oleum intercalation and nitric acid oxidation treatment, while the structure and properties of SWCNTs are preserved. These functionalized CBs have a positive role in the dispersion of SWCNTs. High-performance TCFs with a low sheet resistance of 76 and 133 Ω sq^{-1} at optical transmittance of 82% and 90% were fabricated from these SWCNT suspensions; this superior performance results from the high quality and good dispersion of the SWCNTs.

4. Experimental Section

Preparation of Soluble SWCNTs: For purification of the SWCNTs, Fe catalyst nanoparticles were partly removed by refluxing the as-produced SWCNTs in 37% HCl for 48 h. The as-purified SWCNTs were washed with an abundant amount of water and then vacuum dried at 200 °C for 1 h. Table 1 lists the detailed experimental parameters for the preparation of soluble SWCNTs. Typically, 50 mg as-purified SWCNTs were stirred in 15, 30, and 60 mL oleum (100% H_2SO_4 with 20% SO_3) at 25, 80, and 120 °C for 4 days to ensure good intercalation and disentanglement of SWCNTs. The oleum-SWCNT slurry was then added dropwise to 67% HNO_3 while stirring, with one drop every 1–2 seconds to keep the reaction temperature at 70 ± 5 °C. After adding all the slurry, the reaction lasted for another 1 h. Then, an abundant amount of water was added

dropwise to the mixture of SWCNTs and acids in an oil bath to ensure that the temperature of the mixture was below 75 °C during the whole dilution process. Finally, the soluble SWCNT slurry was obtained by filtrating. [*Caution*: Due to the high corrosivity of the oleum and HNO_3, the above treatment should be done with care in a fume hood.]

Fabrication and Treatment of SWCNT TCFs: The obtained soluble SWCNTs were dispersed in water with a concentration of about 1 mg L^{-1} and used as a filtrate which was subsequently vacuum filtered through a mixed cellulose ester (MCE) membrane with a pore size of 220 nm. The thickness of the TCFs was controlled by the amount of the filtrate. The MCE membrane was transferred to a desired substrate and then the membrane was removed in an acetone bath. The obtained SWCNT film on the substrate was heated in air at 550 °C for 2 min to remove the functionalized CBs, then immersed in 37% HCl for 2 min to remove Fe residues, and finally doped by 67% HNO_3 for 30 min.

Characterization: The SWCNTs were characterized using TEM (JEOL 2010, 200 kV and Tecnai F30, 300 kV), SEM (Nova Nano SEM 430, 18 kV), TGA (Netzsch STA 449 F3), Raman spectroscopy (Labram HR 800 with a 632.8 nm laser), and XPS (ESCALAB 250). In order to compare oleum intercalation conditions and the dispersion efficiency of the soluble SWCNTs, absorption spectroscopy of the soluble SWCNT suspensions was performed by a UV–vis–NIR spectrometer (Varain Cary 5000) as follows: 50 mL water was added in vials containing each soluble SWCNT sample listed in Table 1. After standing for 2 days to form a homogenous suspension, the suspension was filled in a rectangular 10 mm open top quartz cuvette for the absorption spectroscopy measurement. Optical absorption spectra and the transmittance of the SWCNT TCFs were also recorded using this UV–vis–NIR spectrometer. To demonstrate the dispersion state of the SWCNTs in suspensions, samples were prepared for AFM characterization (Veeco MultiMode/NanoScope IIIa, tapping mode) by spreading a drop of diluted SWCNT dispersion over a clean silicon wafer. The samples were then blow dried by nitrogen gas and heated at 350 °C for 10 min in air. The thickness of the SWCNT TCFs was examined by transfering the SWCNT networks onto a clean silicon wafer for AFM observation. The sheet resistance of the SWCNT TCFs was measured by a standard 4-point probe resistivity measurement system (RTS-9, Guangzhou, China).

Supporting Information

Supporting Information is available from the Wiley Online Library or from the author.

Acknowledgements

This work was supported by the National Natural Science Foundation of China (No. 50921004, 90606008 and 50703045), the Key Research Program of Ministry of Science and Technology, China (No. 2011CB932604) and by Chinese Academy Sciences (KJCX2-YW-M01). The authors sincerely thank Prof. Esko I. Kauppinen for his helpful discussions.

Received: January 4, 2011
Published online: May 2, 2011

[1] M. S. Dresselhaus, G. Dresselhaus, P. Avouris, *Carbon Nanotubes: Synthesis, Structure, Properties, and Applications*, Springer, Berlin **2001**.
[2] S. Reich, C. Thomsen, J. Maultzsch, *Carbon Nanotubes: Basic Concepts and Physical Properties*, VCH, Weinheim, Germany **2004**.
[3] L. Vaisman, H. D. Wagner, G. Marom, *Adv. Colloid Interface Sci.* **2006**, *128*, 37.
[4] Z. Chen, K. Kobashi, U. Rauwald, R. Booker, H. Fan, W.-F. Hwang, J. M. Tour, *J. Am. Chem. Soc.* **2006**, *128*, 10568.
[5] L. A. Girifalco, M. Hodak, R. S. Lee, *Phys. Rev. B* **2000**, *62*, 13104.
[6] Y. Asada, Y. Miyata, Y. Ohno, R. Kitaura, T. Sugai, T. Mizutani, H. Shinohara, *Adv. Mater.* **2010**, *22*, 2698.
[7] Y. Noguchi, T. Fujigaya, Y. Niidome, N. Nakashima, *Chem. Eur. J.* **2008**, *14*, 5966.
[8] N. Nakashima, S. Okuzono, H. Murakami, T. Nakai, K. Yoshikawa, *Chem. Lett.* **2003**, *32*, 456.
[9] L. S. Witus, J.-D. R. Rocha, V. M. Yuwono, S. E. Paramonov, R. B. Weisman, J. D. Hartgerink, *J. Mater. Chem.* **2007**, *17*, 1909.
[10] J. Y. Hwang, A. Nish, J. Doig, S. Douven, C. W. Chen, L. C. Chen, R. J. Nicholas, *J. Am. Chem. Soc.* **2008**, *130*, 3543.
[11] Y. Yamamoto, T. Fujigaya, Y. Niidome, N. Nakashima, *Nanoscale* **2010**, *2*, 1767.
[12] M. Zheng, A. Jagota, E. D. Semke, B. A. Diner, R. S. Mclean, S. R. Lustig, R. E. Richardson, N. G. Tassi, *Nat. Mater.* **2003**, *2*, 338.
[13] M. J. O'Connell, S. M. Bachilo, C. B. Huffman, V. C. Moore, M. S. Strano, E. H. Haroz, K. L. Rialon, P. J. Boul, W. H. Noon, C. Kittrell, J. P. Ma, R. H. Hauge, R. B. Weisman, R. E. Smalley, *Science* **2002**, *297*, 593.
[14] S. Banerjee, T. Hemraj-Benny, S. S. Wong, *Adv. Mater.* **2005**, *17*, 17.
[15] J. N. Coleman, *Adv. Funct. Mater.* **2009**, *19*, 3680.
[16] S. Giordani, S. D. Bergin, V. Nicolosi, S. Lebedkin, M. M. Kappes, W. J. Blau, J. N. Coleman, *J. Phys. Chem. B* **2006**, *110*, 15708.
[17] C. A. Furtado, U. J. Kim, H. R. Gutierrez, L. Pan, E. C. Dickey, P. C. Eklund, *J. Am. Chem. Soc.* **2004**, *126*, 6095.
[18] X. L. Li, L. Zhang, X. R. Wang, I. Shimoyama, X. M. Sun, W. S. Seo, H. J. Dai, *J. Am. Chem. Soc.* **2007**, *129*, 4890.
[19] Y. Wang, C. A. Di, Y. Q. Liu, H. Kajiura, S. H. Ye, L. C. Cao, D. C. Wei, H. L. Zhang, Y. M. Li, K. Noda, *Adv. Mater.* **2008**, *20*, 4442.
[20] D. S. Kim, D. Nepal, K. E. Geckeler, *Small* **2005**, *1*, 1117.
[21] X. Y. Zhang, A. C. Coleman, N. Katsonis, W. R. Browne, B. J. van Wees, B. L. Feringa, *Chem. Commun.* **2010**, *46*, 7539.
[22] A. C. Dillon, T. Gennett, K. M. Jones, J. L. Alleman, P. A. Parilla, M. J. Heben, *Adv. Mater.* **1999**, *11*, 1354.
[23] F. Li, H. M. Cheng, Y. T. Xing, P. H. Tan, G. Su, *Carbon* **2000**, *38*, 2041.
[24] I. W. Chiang, B. E. Brinson, R. E. Smalley, J. L. Margrave, R. H. Hauge, *J. Phys. Chem. B* **2001**, *105*, 1157.
[25] F. Lu, X. Wang, M. J. Meziani, L. Cao, L. Tian, M. A. Bloodgood, J. Robinson, Y.-P. Sun, *Langmuir* **2009**, *26*, 7561.
[26] C. G. Salzmann, S. A. Llewellyn, G. Tobias, M. A. H. Ward, Y. Huh, M. L. H. Green, *Adv. Mater.* **2007**, *19*, 883.
[27] J. Kim, L. J. Cote, F. Kim, W. Yuan, K. R. Shull, J. Huang, *J. Am. Chem. Soc.* **2010**, *132*, 8180.
[28] Q. Liu, W. Ren, Z.-G. Chen, D.-W. Wang, B. Liu, B. Yu, F. Li, H. Cong, H.-M. Cheng, *ACS Nano* **2008**, *2*, 1722.
[29] H. M. Cheng, F. Li, G. Su, H. Y. Pan, L. L. He, X. Sun, M. S. Dresselhaus, *Appl. Phys. Lett.* **1998**, *72*, 3282.
[30] S. Ramesh, L. M. Ericson, V. A. Davis, R. K. Saini, C. Kittrell, M. Pasquali, W. E. Billups, W. W. Adams, R. H. Hauge, R. E. Smalley, *J. Phys. Chem. B* **2004**, *108*, 8794.
[31] N. Behabtu, J. R. Lomeda, M. J. Green, A. L. Higginbotham, A. Sinitskii, D. V. Kosynkin, D. Tsentalovich, A. N. G. Parra-Vasquez, J. Schmidt, E. Kesselman, Y. Cohen, Y. Talmon, J. M. Tour, M. Pasquali, *Nat. Nanotechnol.* **2010**, *5*, 406.
[32] L. M. Ericson, H. Fan, H. Q. Peng, V. A. Davis, W. Zhou, J. Sulpizio, Y. H. Wang, R. Booker, J. Vavro, C. Guthy, A. N. G. Parra-Vasquez, M. J. Kim, S. Ramesh, R. K. Saini, C. Kittrell, G. Lavin, H. Schmidt, W. W. Adams, W. E. Billups, M. Pasquali, W. F. Hwang, R. H. Hauge, J. E. Fischer, R. E. Smalley, *Science* **2004**, *305*, 1447.
[33] B. Zhao, H. Hu, R. C. Haddon, *Adv. Funct. Mater.* **2004**, *14*, 71.
[34] M. N. Tchoul, W. T. Ford, G. Lolli, D. E. Resasco, S. Arepalli, *Chem. Mater.* **2007**, *19*, 5765.
[35] W. Zhao, C. Song, P. E. Pehrsson, *J. Am. Chem. Soc.* **2002**, *124*, 12418.

[36] J. Zhu, J. Kim, H. Peng, J. L. Margrave, V. N. Khabashesku, E. V. Barrera, *Nano Lett.* **2003**, *3*, 1107.
[37] L. Jie, A. G. Rinzler, D. Hongjie, J. H. Hafner, R. K. Bradley, P. J. Boul, A. Lu, T. Iverson, K. Shelimov, C. B. Huffman, F. Rodriguez-Macias, S. Young-Seok, T. R. Lee, D. T. Colbert, R. E. Smalley, *Science* **1998**, *280*, 1253.
[38] M. S. Dresselhaus, G. Dresselhaus, *Adv. Phys.* **1981**, *30*, 139.
[39] S. H. Jeong, K. K. Kim, S. J. Jeong, K. H. An, S. H. Lee, Y. H. Lee, *Synth. Met.* **2007**, *157*, 570.
[40] M. E. Itkis, D. E. Perea, S. Niyogi, S. M. Rickard, M. A. Hamon, B. Zhao, R. C. Haddon, *Nano Lett.* **2003**, *3*, 309.
[41] P. N. Nirmalraj, P. E. Lyons, S. De, J. N. Coleman, J. J. Boland, *Nano Lett.* **2009**, *9*, 3890.
[42] A. Yu, C.-C. L. Su, I. Roes, B. Fan, R. C. Haddon, *Langmuir* **2009**, *26*, 1221.
[43] H. Z. Geng, K. K. Kim, C. Song, N. T. Xuyen, S. M. Kim, K. A. Park, D. S. Lee, K. H. An, Y. S. Lee, Y. Chang, Y. J. Lee, J. Y. Choi, A. Benayad, Y. H. Lee, *J. Mater. Chem.* **2008**, *18*, 1261.
[44] A. Kaskela, A. G. Nasibulin, M. Y. Timmermans, B. Aitchison, A. Papadimitratos, Y. Tian, Z. Zhu, H. Jiang, D. P. Brown, A. Zakhidov, E. I. Kauppinen, *Nano Lett.* **2010**, *10*, 4349.
[45] M. S. Dresselhaus, G. Dresselhaus, R. Saito, A. Jorio, *Phys. Rep.* **2005**, *409*, 47.
[46] K. H. An, J. G. Heo, K. G. Jeon, D. J. Bae, C. Jo, C. W. Yang, C.-Y. Park, Y. H. Lee, Y. S. Lee, Y. S. Chung, *Appl. Phys. Lett.* **2002**, *80*, 4235.
[47] T. I. T. Okpalugo, P. Papakonstantinou, H. Murphy, J. McLaughlin, N. M. D. Brown, *Carbon* **2005**, *43*, 153.
[48] R. Graupner, J. Abraham, A. Vencelova, T. Seyller, F. Hennrich, M. M. Kappes, A. Hirsch, L. Ley, *Phys. Chem. Chem. Phys.* **2003**, *5*, 5472.
[49] Z. C. Wu, Z. H. Chen, X. Du, J. M. Logan, J. Sippel, M. Nikolou, K. Kamaras, J. R. Reynolds, D. B. Tanner, A. F. Hebard, A. G. Rinzler, *Science* **2004**, *305*, 1273.
[50] R. Jackson, B. Domercq, R. Jain, B. Kippelen, S. Graham, *Adv. Funct. Mater.* **2008**, *18*, 2548.
[51] H. Tantang, J. Y. Ong, C. L. Loh, X. C. Dong, P. Chen, Y. Chen, X. Hu, L. P. Tan, L. J. Li, *Carbon* **2009**, *47*, 1867.
[52] L. Hu, D. S. Hecht, G. Gruner, *Nano Lett.* **2004**, *4*, 2513.
[53] S. De, J. N. Coleman, *ACS Nano* **2010**, *4*, 2713.
[54] P. J. King, U. Khan, M. Lotya, S. De, J. N. Coleman, *ACS Nano* **2010**, *4*, 4238.
[55] S. F. Pei, J. H. Du, Y. Zeng, C. Liu, H. M. Cheng, *Nanotechnology* **2009**, *20*, 235707.
[56] M. S. Strano, *J. Am. Chem. Soc.* **2003**, *125*, 16148.
[57] R. B. Weisman, S. M. Bachilo, *Nano Lett.* **2003**, *3*, 1235.
[58] X. Tu, S. Manohar, A. Jagota, M. Zheng, *Nature* **2009**, *460*, 250.